Landslides (2022) 19:719–729
DOI 10.1007/s10346-021-01727-0
Received: 27 January 2021
Accepted: 17 June 2021
Published online: 7 January 2022

Honghui Wang · Pan Zhong · Dehao Xiu · Yunshun Zhong · Dalei Peng · Qiang Xu

Monitoring tilting angle of the slope surface to predict loess fall landslide: an on-site evidence from Heifangtai loess fall landslide in Gansu Province, China

Abstract Due to the huge losses caused by landslides, landslide deformation monitoring has become essential. The change of the tilting angle of the slope surface can reflect the instability process of the landslide. However, there are few studies on the relationship between the instability process of landslides and the tilting angle of the slope surface on the time scale. Therefore, there are even fewer cases in using the inclination angle of the landslide as an early warning method in practice. On August 24, 2018, a wireless tilt sensor network was deployed in the Heifangtai area of Gansu Province in China, to monitor the inclination state of loess landslides to study the relationship between the tilting angle of the slope surface and the landslide instability process. At 4 o'clock on October 5, 2019, the wireless tilt sensor network mentioned above detected a new loess fall landslide. Through the analysis of the monitoring data from the tilting sensor nodes named T3 and T4, we found that the tilting angle of the landslide surface in the pre-sliding stage has significant change compared with the stable stage, which directly verifies that the inclination data can be used for landslide warning. At the same time, we inputted the monitored inclination data into the inclination warning model proposed by Xie et al. (Landslides 17:301–312, 2020) for verification and found that the trend of inclination changes matches the model well. However, the forecast time error is large. Therefore, this paper optimizes the inclination early warning model proposed by Xie. Using the optimized early warning model, the predicted landslide occurrence time based on the data of the T3 node was 0.517 days, which was about 8 h later than the actual landslide that occurred on October 4, 2019, which is an improvement of forecasting. This case serves as an on-site direct evidence to further verify the feasibility of using the landslide body inclination state as a landslide monitoring and early warning parameter which can be promoted and used in practice.

Keywords: Loess fall landslide monitoring · Tilting angle · Early warning model · Wireless sensor network

Introduction

Landslides are one of the most common types of geological disasters in the world (Brabb 1991; Nadim et al. 2006). Landslides cause thousands of deaths and billions of dollars in losses every year on earth (Robinson and Spieker 1978; Lu et al. 2007). To reduce the losses caused by landslides, various landslide monitoring devices are used all over the world to monitor landslides, and many scholars have also proposed many early warning models (Pecoraro et al. 2018; Fan et al. 2019).

Aiming at loess landslides monitoring and early warning, researchers also have done significant works. Peng et al. (2014) suggested that we should study and explore the technical methods for high-precision monitoring of single loess landslide disaster information, and establish a collaborative early warning model that combines multi-source observation data, different time and space scales, multiple early warning models, and early warning indicators. Zhao et al. (2016) used small baseline subsets interferometric synthetic aperture radar technique to detect and monitor the loess landslide in the southern bank of the Jinghe River, Shaanxi Province, China. The multi-temporal InSAR technique has also been adopted to obtain the loess landslide's continuous earth surface deformation with long time scale and wide geographical coverage (Liu et al. 2016). Xu et al. (2020) studied the theory and method of monitoring and early warning for sudden loess landside and given a case study at Heifangtai terrace, Gansu Province, China. They developed an adaptive intelligent frequency conversion crack meter to capture the displacement data of the loess landslide when the deformation suddenly increased. Furthermore, they established an early warning model based on the displacement rate threshold and the tangent angle, and successfully warned 6 loess landslides.

However, in the existing literature, there are not many studies on the tilting-based approach for landslide disaster monitoring and early warning compared with the above-mentioned monitoring methods. Taro Uchimura's team is working on this problem; such as, Taro Uchimura et al. (2010) used tilt sensors on the slope surface to detect abnormal deformation and indicated that tilt angle can be used for early warning. However, his team did not develop a landslide mathematical model for early warning of body inclination data. Taro Uchimura et al. (2015) conducted field experiments in China and Japan and found that the use of landslide body angle data for monitoring and early warning not only depends on the local landslide conditions but also depends on the location of the tilt sensors. Unfortunately, no warning model is given. Based on the model test, Xie et al. (2020) gave a mathematical model of early warning. The sliding time is determined by the deformation rate and the B value. Here, B is the angular coefficient derived from the linear relation between the reciprocal tilting rate and time by three typical types of laboratory model tests and a field test.

In order to monitor the tilting angle of landslide and find the relationship between the tilting angle with the life expectancy of the landslide, since August 24, 2018, based on the idea of wireless sensor networks (Lin et al. 2008), we have established a landslide body inclination monitoring system in the Heifangtai area of Gansu Province, China, to continuously monitor the tilting angle of the slope surface in the region. Based on the monitoring data from April 5, 2019, to October 5, 2019, we carried out (1) analysis of monitoring data to verify the practical feasibility of the tilting angle for landslide warning; (2) calculating the critical sliding time based on the tilting early warning model that Xie proposed (Xie et al. 2020); (3) optimizing the existing tilting early warning model in (2) to improve the timeliness of forecasting.

The remainder of this paper is organized as follows. The "2" section introduces the system we used in the study area that includes tilting sensor nodes, the gateway, and the visualization platform. The "8" section describes the study area. The "9" section describes the final result of the landslide we monitored, discusses the data monitored by the tilting sensor nodes, and uses an early warning model to validate the monitored data. Then, the model is improved and data analysis is performed. Finally, the conclusions are presented in the "13" section.

Methodology

This landslide inclination monitoring system can be divided into three parts: tilting sensor node, gateway, and visualization platform. The architecture of the entire system is shown in Fig. 1.

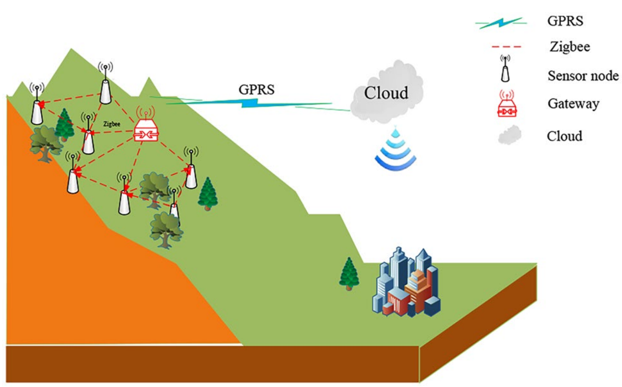

Fig. 1 The diagram of the system structure. The tilting sensor nodes transmit the monitored data to the gateway node via wireless link using Zigbee protocol (2.4 GHz). The gateway node sends the data to the visualization platform via GPRS. Of course, the commands are issued through the opposite link. That is, the visualization platform sends the commands to the gateway, and then the gateway forwards the commands to the tilt sensor nodes

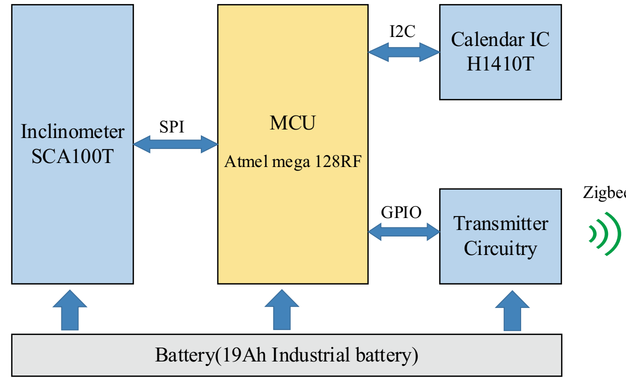

Fig. 2 Block diagram of the tilting sensor node

Tilting sensor node

Through the tilting sensor nodes, we can get the tilting angle of the slope surface. The structure of the tilting sensor node is shown in Fig. 2.

As shown in Fig. 2, the tilting sensor node is comprised of five components. The main component is the Micro-Controller Unit (MCU). The calendar Integrated Circuit (IC) which provides the time information is connected to the MCU via Inter-Integrated Circuit (I2C) bus. The tilt sensor samples the tilting angle and transmits it to the MCU through the Serial Peripheral Interface (SPI) bus. All the components are powered by the 19Ah industrial battery.

With the development of the Micro Electro Mechanical System (MEMS) technology, sensors can be made smaller and lighter. In this paper, we use the MEMS-based tilt sensor (SCA100T-D01 and its measurement range is ± 30°). The tilting sensor node contains an Application Specific Integrated Circuit (ASIC) and a silicon sensitive micro capacitance sensor. The ASIC circuit is composed of memory, signal amplifier, analog to digital converter, temperature sensor, and SPI interface, which forms a completely digital application tilt sensor.

The tilting sensor node is shown in Fig. 3d, and its reading reference diagram is shown in Fig. 3a–c.

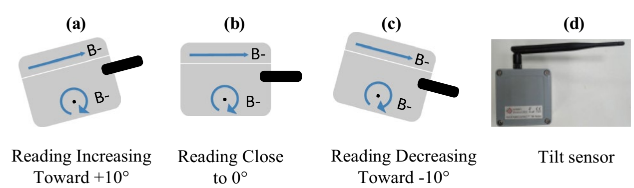

Fig. 3 (**a**–**c**) Readings of tilt sensor node. (**d**) Image of tilt sensor node

Table 1 Parameter specifications of the tilt sensor node and gateway

Equipment type	Inclination sensor node	Gateway
Size	80 × 75 × 57 mm	180 × 140 × 60 mm
Standard wireless interface	2.4 GHz	Compatible with 2G/2.5G/3G/4G (micro SIM card)
Weight	0.43 kg	≤ 2.0 kg
Protection level	IP66	IP66
Working temperature range	−40 to 80 °C	−40 to 80 °C

Gateway

As the hub connecting the tilting sensor node and the visualization platform, the gateway plays an irreplaceable role. The role of the gateway is reflected in two aspects. One is to gather the on-site tilt node data through 2.4-GHz radio frequency waves; the other is to transmit the aggregated data to the visualization platform through the GPRS communication link for long-distance inclination state monitor of the slope surface.

The parameter specifications of the tilting sensor node and gateway are shown in Table 1.

Visualization platform

As a platform for interacting with customers, the system visualization platform should be able to select projects, view data, download data, issue early warnings, and issue instructions to the sensor nodes in the system, as shown in Fig. 4.

Figure 4a is the project selection interface of the visualization platform, in which users can choose their projects. After entering the project, users can view the battery voltage, temperature, tilting angle data, and network parameters of each node (Fig. 4b). At the same time, the platform also has a data graphing function, in which customers can directly view the trend of monitoring parameters on the platform, as shown in Fig. 4c. In addition, customers can give orders to all nodes in the project on the platform, such as modifying the data collection time and network access threshold (shown in Fig. 4d).

Study area

On August 24, 2018, we deployed the landslide inclination monitoring system in the Heifangtai area of Gansu Province, China, to monitor the tilting angle of the slope surface. Heifangtai is located in the Liupanxia Reservoir area, Yongjing County, Gansu Province in Northwest China, which is 45 km away from Lanzhou City and 20 km away from Yongjing County. The location of the Heifangtai region is shown in Fig. 5a.

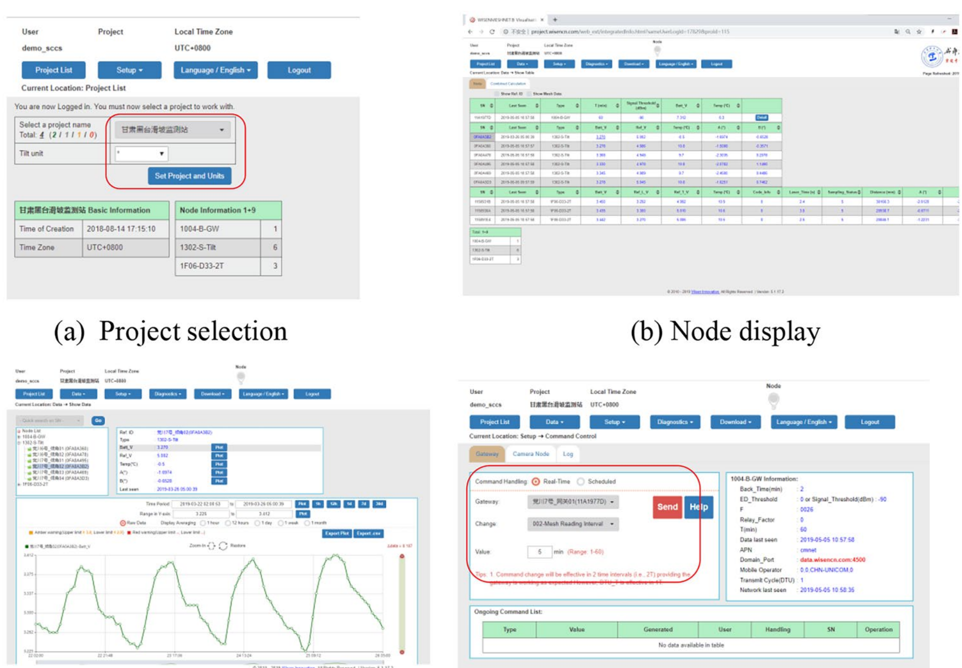

(a) Project selection

(b) Node display

(c) Data display

(d) Sending instruction

Fig. 4 Images of visualization platform: (**a**) project selection, (**b**) node display, (**c**) data display, (**d**) sending instruction

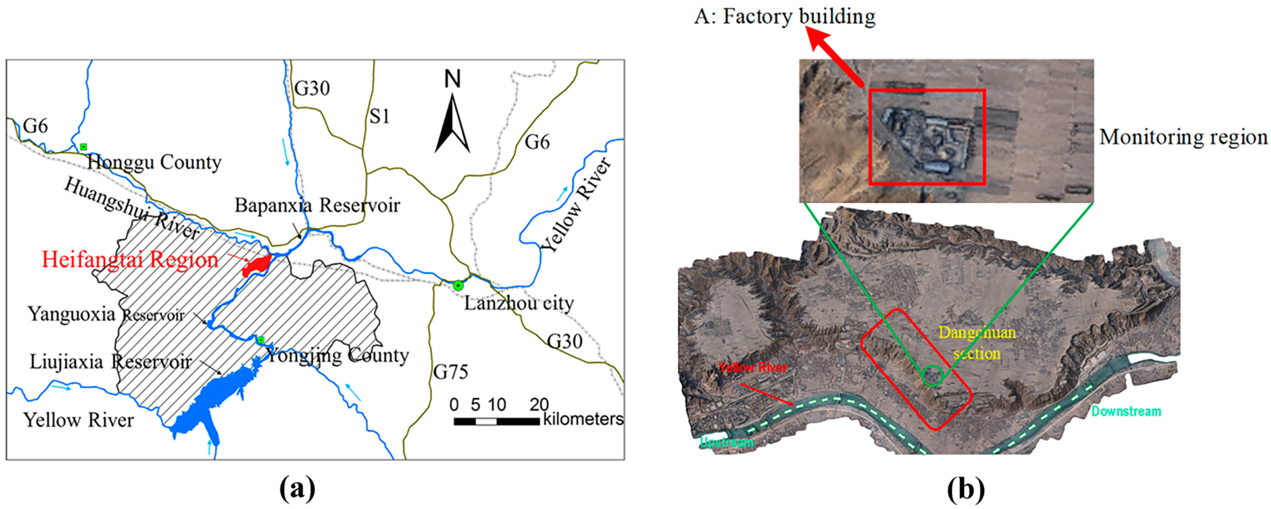

Fig. 5 (**a**) The location of the Heifangtai region. (**b**) The location of the Dangchuan section in the Heifangtai region

The Heifangtai region was once an uninhabited dry platform, and the long-term pumping water and irrigation for the crops on the platform broke the ecological environment balance of the region (Qi et al. 2016) which changed the geological environmental conditions. Due to the water content sensitivity of the loess itself, a large amount of Yellow River water irrigated on the platform caused the platform to collapse and crack. Therefore, it induced a large number of landslides around the platform edge (Qi et al. 2018), and seriously endangered the sustainable development of the local economy and the safety of nearby villagers.

Based on field survey and experimental data, the loess belongs to Malan Loess (Q_3^{eol}), and its physical and geotechnical properties are shown in Table 2.

Table 2 The physical and geotechnical properties of the loess

Parameter		Symbol	Unit	Value
Dry density		ρ_d	g/cm^3	1.41
Natural density		ρ	g/cm^3	1.65
Specific gravity		G_S	g/cm^3	2.72
Natural water content		w	%	16.9
Void ratio		e	-	0.93
Plastic limit		W_P	%	15.8
Liquid limit		W_L	%	28.2
Plasticity index		IP	%	12.4
Horizontal permeability		K_h	mm/day	154
Vertical permeability		K_v	mm/day	218
Grain size distribution		< 0.005 mm	%	17.39
		0.005 ~ 0.075 mm	%	79.79
		> 0.075 mm	%	2.82
Shear strength	Natural state	c	kPa	50
		Φ	°	23
	Saturated state	c	kPa	9
		Φ	°	7

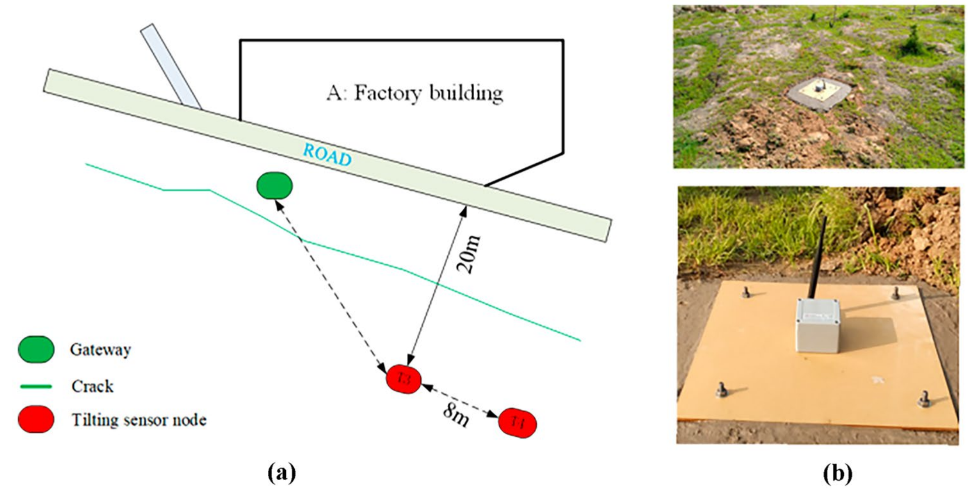

Fig. 6 The deployment position of the two tilting sensor nodes

As shown in Fig. 5b, the Dangchuan area is located on the edge of the southwest plateau of Heifangtai, and two tilting sensor nodes are deployed in the Dangchuan area. Figure 6 shows the installation location of tilting sensor nodes named T3 and T4.

Results and discussion

Heifangtai loess fall landslide summary

At 4 o'clock on October 5, 2019, a loess fall landslide occurred in the monitoring area. The scope of the landslide and its scene are shown in Fig. 7. The failure source area is 58 m long and 107 m wide, and the displaced material travelled 355 m (horizontal distance). The total volume of the landslide is approximately 40,000 m^3, and the two tilting sensor nodes (T3 and T4 marked as white triangle) have detected significant inclination changes of the slope surface.

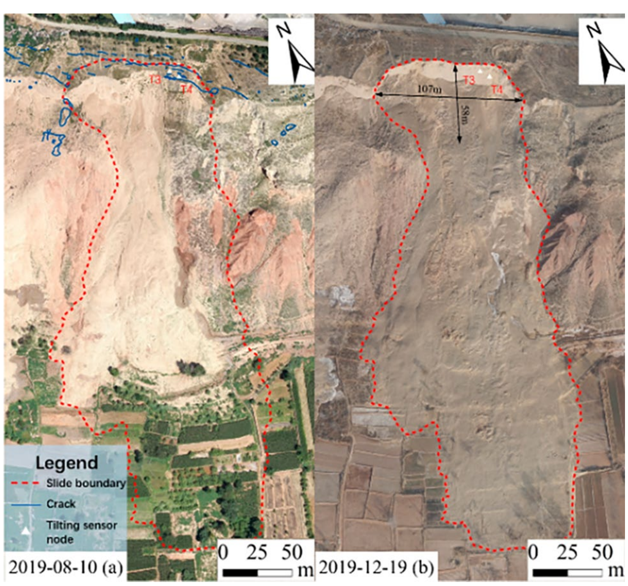

Fig. 7 Images of the landslide. (**a**) The remote sensing image before failure. (**b**) The remote sensing image after failure

Based on the investigation and summary of the same type of landslide in the study area, the failure mode map of this kind of landslide can be drawn as Fig. 8. Firstly, under the influence of previous landslide in 2014, the landslide produced a large number of unloading crown cracks. Secondly, with the effect of self weight, the crack expands downward, which makes the crown gradually produce steps and produce a certain angle of ground surface tilt. According to the installation mode of tilting sensor nodes, the increase of tilting angle indicates that the slope is gradually leaned back down, which conforms to the shape of the surface of rupture.

Figure 9 shows the data from two tilting sensor nodes (unit: °). The angle monitored by the T3 node has increased from 0.415 to 0.882° (Fig. 9a), an increase of 0.467°. The angle monitored by the T4 node increased from 0.691 to 1.861°, an increase of 1.170° (Fig. 9b).

The angle values monitored by the two tilting sensor nodes have detected significant changes in the landslide body 5 days before the occurrence of the landslide. In these five days of the landslide, the angle of the T3 node changed by 0.346° ($0.882° - 0.536° = 0.346°$), accounting for 74.09% of the total change ($0.346°/0.467° \times 100\% = 74.09\%$); the angle monitored by the T4 node changed by 0.855° ($1.861° - 1.026° = 0.855°$), accounting for 73.08% of the total change ($0.855°/1.170° \times 100\% = 73.08\%$). And it can be seen from Fig. 9 that the closer the critical sliding time, the greater the angle change. Therefore, it is feasible to use the inclination state of the slope surface as a landslide early warning parameter according to the qualitative analysis of the monitoring data.

It should be mentioned that the tilting angle from the T3 node is highly oscillating (Fig. 9a). This is because the sensor node is installed on the acrylic plate and only fixed on the surface of the landslide. Reading is affected by the deformation of the acrylic sheet, which is caused by the large temperature difference between day and night in the monitoring area. In addition, the other environmental factor, especially rainfall, may cause local deformation of the loess around the sensor node, resulting in data shaking that cannot be filtered out. In order to overcome this limitation, we can choose a more robust pallet to fix the angle sensors. Besides, we can fix the sensors with the long rod embedded into the loess to reduce the influence of rainfall.

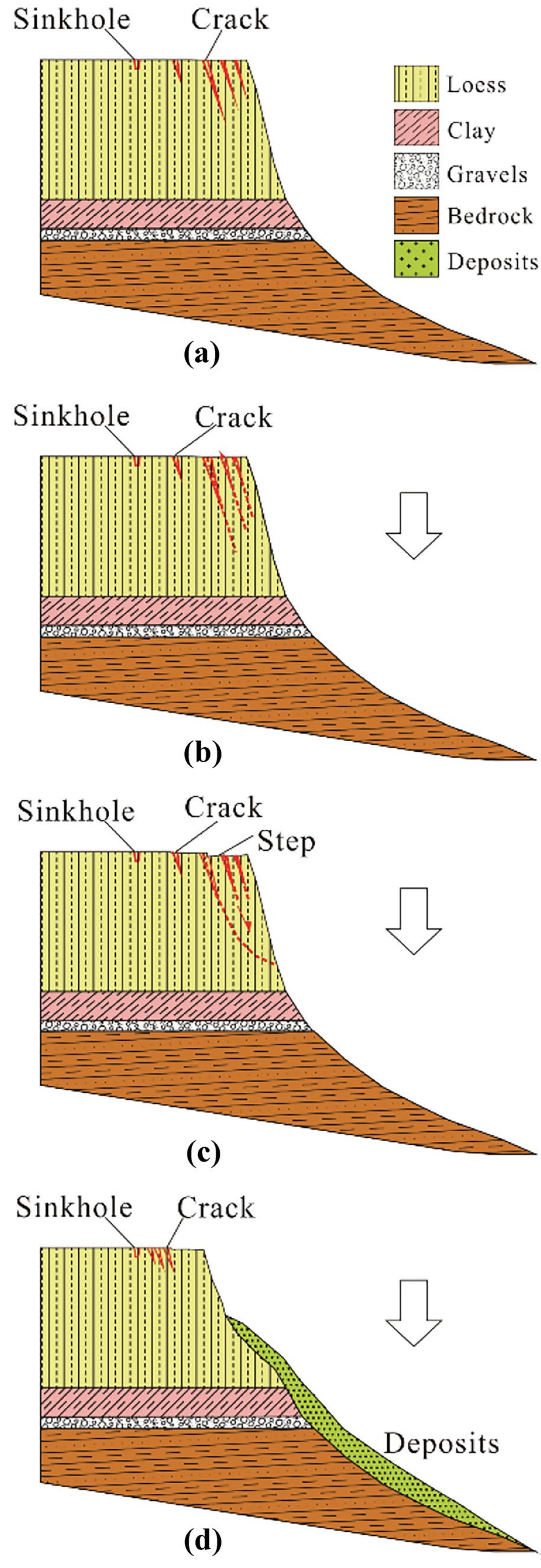

Fig. 8 The failure mode

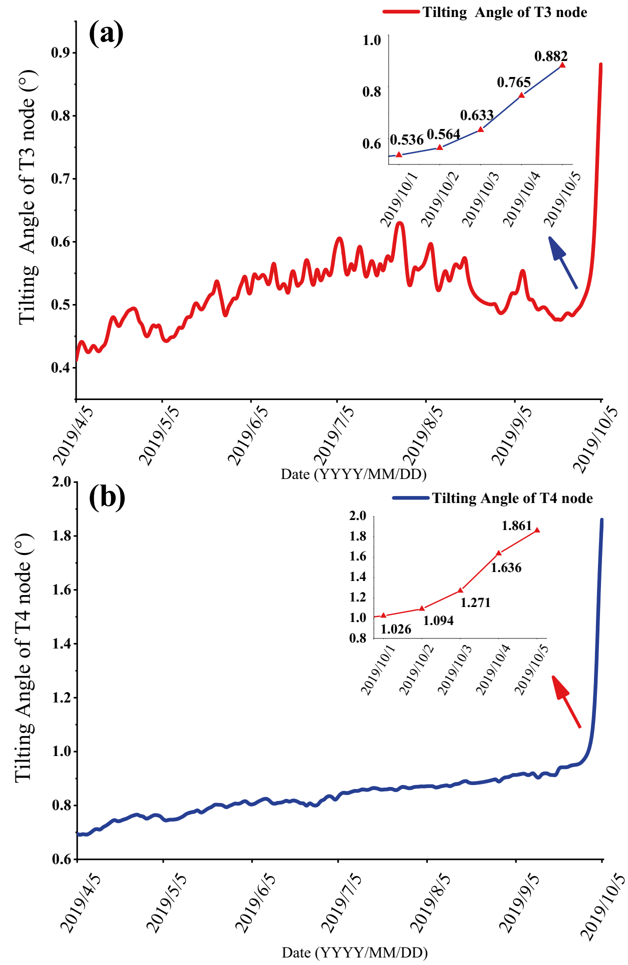

Fig. 9 Image of the data. (**a**) Tilting angle of the T3 node. (**b**) Tilting angle of the T4 node

Monitoring data analysis

In this case, we select the data from 2019/4/5 to 2019/10/5 for analysis. Figure 10 shows the inclination state of the slope surface and the rate of inclination change (unit: °/day).

It can be seen from Fig. 10 that the two tilting sensor nodes have detected abrupt changes in the tilting angle of the slope surface, and the rate of change of the tilting angle monitored by the T3 node increased from 0 to 0.13°/day (Fig. 10c). The rate of change of the tilting angle monitored by the T4 node increased from 0 to 0.365°/day (Fig. 10d). Especially in 2019/10/2 and later, the tilting angle change rate of the T3 node changes from 0.028 to 0.069°/day in 2019/10/3, and the tilting angle change rate of the T4 node changes from 0.068 to 0.177°/day on October 3, 2019, and then on October 4, 2019, the rate of change of the T4 node sharply increased to 0.365°/day, and the rate of change of the T3 node sharply increased to 0.132°/day.

From the above analysis, it can be seen that the inclination data monitored by the two tilting sensor nodes show a different rate of change during the critical sliding period than the past. Therefore, it is effective in practice to use the inclination state of the slope

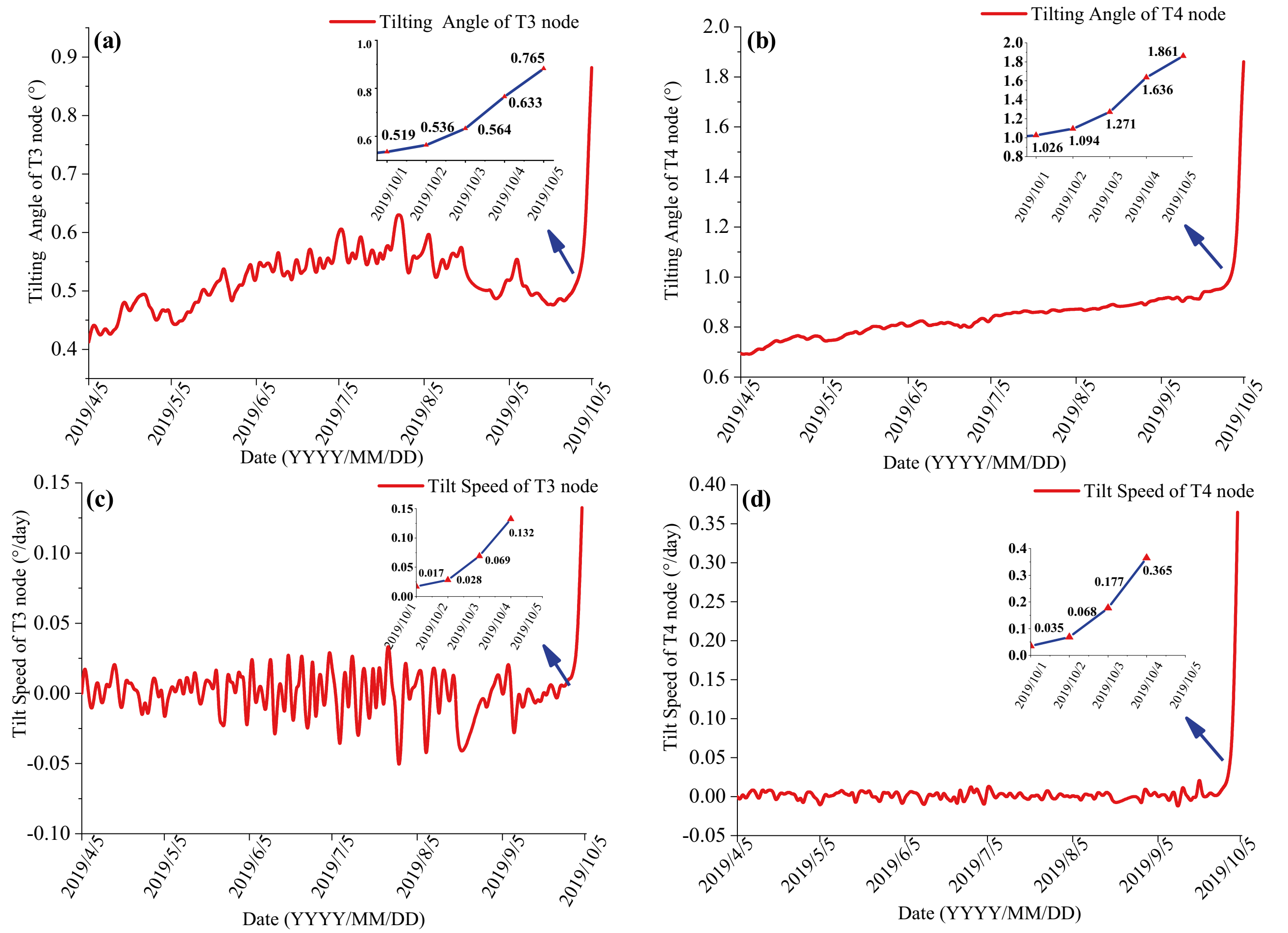

Fig. 10 (**a**) The tilting angle of the T3 node. (**b**) The tilting angle of the T4 node. (**c**) The tilting speed of the T3 node. (**d**) The tilting speed of the T4 node

surface as a warning parameter. This case serves as an on-site direct evidence to further verify the feasibility of using the slope surface inclination state as a landslide monitoring and early warning parameter.

Critical sliding time calculating

Xie et al. (2020) proved the feasibility of tilting angle for landslide warning through a series of experiments and proposed a method to predict the occurrence of slope failure. However, the method was just validated in the laboratory but not in the actual landslides. In this case, we choose the model that the literature (Xie et al. 2020) proposed for landslide early warning forecasts. In the paper mentioned above, the linear correlation between the reciprocal tilting rate and time in the acceleration stage of tilting is shown as Eq. 1.

$$\frac{dt}{|d\theta|} = \frac{-t}{B} + \frac{t_f}{B} \tag{1}$$

where $\frac{dt}{|d\theta|}$ is the inverse number of tilting rates, and t means time. B is the angular coefficient derived from the linear relation between the reciprocal tilting rate and time. t_f represents the slope failure time. Xie et al. gave a suggested range for the value of B: [0.5, 1.99] from their calculations. To simplify the calculation, we can get Eq. 2.

$$\frac{|d\theta|}{dt} \cdot t_d = B \tag{2}$$

where $\frac{|d\theta|}{dt}$ means the tilting rate (in °/day) and t_d represents the duration (in day), which indicates the critical sliding time of the landslide. It can be seen from Eq. 2 that when $\frac{|d\theta|}{dt}$ is a certain value, the larger the value of B, the larger t_d. In this case, we first take the minimum value of 0.5 for calculation. Figure 11 shows the change of life expectancy and the tilting rate over time when B is 0.5.

The tilting rate of the T3 node on 3 October 2019 is 0.069°/day. The corresponding life expectancy is 7.235 (day). Furthermore, the tilting rate of the T3 node on 4 October 2019 is 0.132°/day. The corresponding life expectancy is 3.778 (day). Similarly, the tilting rate of the T4 node on 3 October 2019 is 0.177°/day. The corresponding life expectancy is 2.826 (day). Furthermore, the tilting rate of the T4 node on 4 October 2019 is 0.365°/day. The corresponding life expectancy is 1.371 (day).

It can be seen from Fig. 11b that the landslide instability time was 1.371 days, or 32.904 h according to the data monitored by the

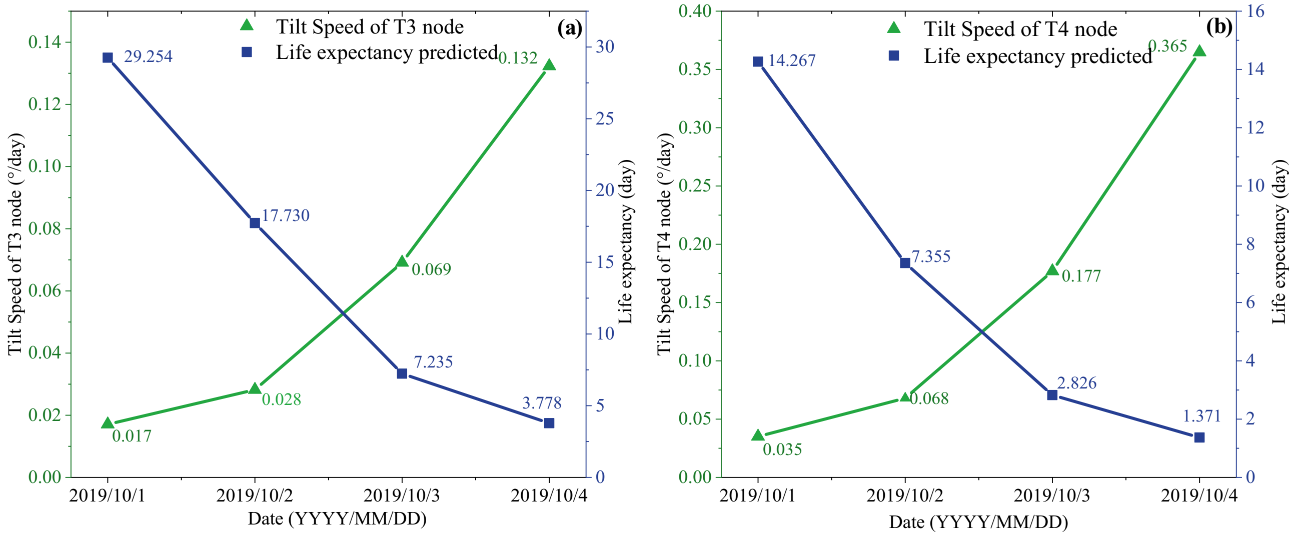

Fig. 11 The tilting rate and the life expectancy predicted based on (**a**) the T3 node and (**b**) the T4 node

T4 node, on 2019/10/4. However, the landslide occurred at 4:00 on October 5, which was about 29 h away from the predicted time. The landslide instability time error obtained from the data monitored by the T3 node is even greater. As shown in Fig. 11a, the landslide instability time was 3.778 days on 2019/10/4, which is 90.672 h. It is about 86 h away from the predicted time. However, the value of B is already at a minimum value of 0.5, and B has a positive correlation with the warning time. If the value of B is larger, the error will be even larger, as shown in Table 3.

Although the time trend predicted by the above model is consistent with the actual situation, the error is relatively large according to the analysis above. Therefore, we need to have a try to optimize the early warning model.

Tilting angle early warning model optimization

It can be seen from Fig. 11 that for different locations of the same landslide, the deformation rate is different, and the B value should also be different. Since the value of B is different for different landslides, the value of B should be related to the historical inclination changes monitored at a specific monitoring point of the landslide.

Table 3 The relationship between B value and warning time

B	T3 life expectancy (day)	T4 life expectancy (day)	T3 life expectancy difference (day)	T4 life expectancy difference (day)
0.5	3.778	1.371	3.611	1.204
0.8	6.060	2.192	5.893	2.025
1.1	8.333	3.014	8.166	2.847
1.4	10.606	3.836	10.439	3.669
1.7	12.879	4.658	12.712	4.491
1.99	15.076	5.452	14.909	5.285

When the inclination deformation rate is larger than twice the previous average rate or there is an unprecedented maximum rate, the landslide is considered to be in a state of critical sliding (Yue 2014). For example, it can be seen from Fig. 10 that on October 1, 2019, the landslide entered the critical sliding stage. It can be seen from Fig. 11 that before the occurrence of the landslide, the angle increased multiple (2 to 3) times. Therefore, we change the value of B in Eq. 2 to $C \cdot V_0$, in which V_0 is the initial speed of the acceleration phase and C is a constant, to obtain Eq. 3:

$$t_d = \frac{C \cdot V_0}{\frac{d\theta}{dt}} \tag{3}$$

In this case, we take C equals to 4, the V_0 value of the T3 node equals to 0.017, and the V_0 value of the T4 node is 0.035 to get Fig. 12. It can be seen from Fig. 12 that after adjusting the value of B, the error of t_d is reduced. At the same time, the value of B can reflect the characteristics of the inclination change of each specific monitoring point, making the life expectancy predicted difference by each monitoring point smaller and more accurate.

As shown in Fig. 13, On October 3, 2019, the life expectancy predicted based on the T3 node was 0.989 days in the optimized model proposed in this article and the life expectancy predicted based on the T4 node was 0.792 days. In the unoptimized model, the life expectancy predicted based on the T3 node was 7.235 days and the life expectancy predicted based on the T4 node was 2.826 days. Moreover, on October 4, 2019, the life expectancy predicted based on the T3 node was 0.517 days, and T4 node-based was 0.384 days in the optimized model. In the unoptimized model, the T3 node-based life expectancy was 3.778 days and the T4 node-based life expectancy was 1.371 days. The above data analysis shows that compared with the existing early warning model, the life expectancy predicted by the optimized model is closer to the actual sliding time.

In addition, the life expectancy predicted based on the two monitoring points has relatively large differences in the unoptimized model (Fig. 14).

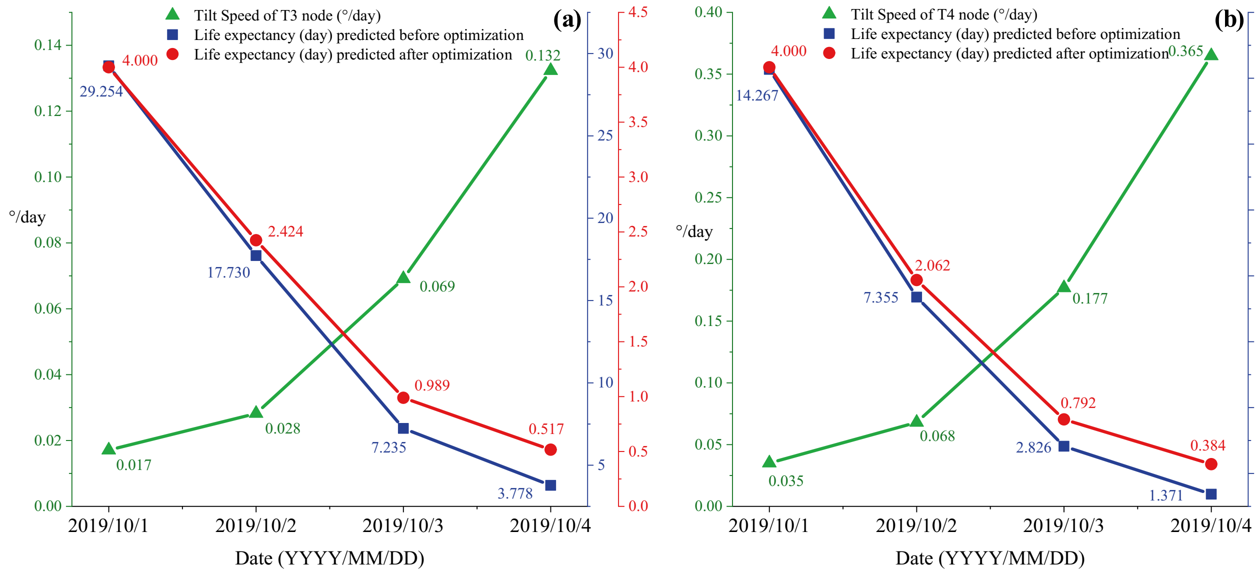

Fig. 12 Comparison between the life expectancy predicted before and after optimization based on (**a**) the T3 node and (**b**) the T4 node

Fig. 13 Comparison between the life expectancy predicted and the actual sliding time based on (**a**) the T3 node and (**b**) the T4 node

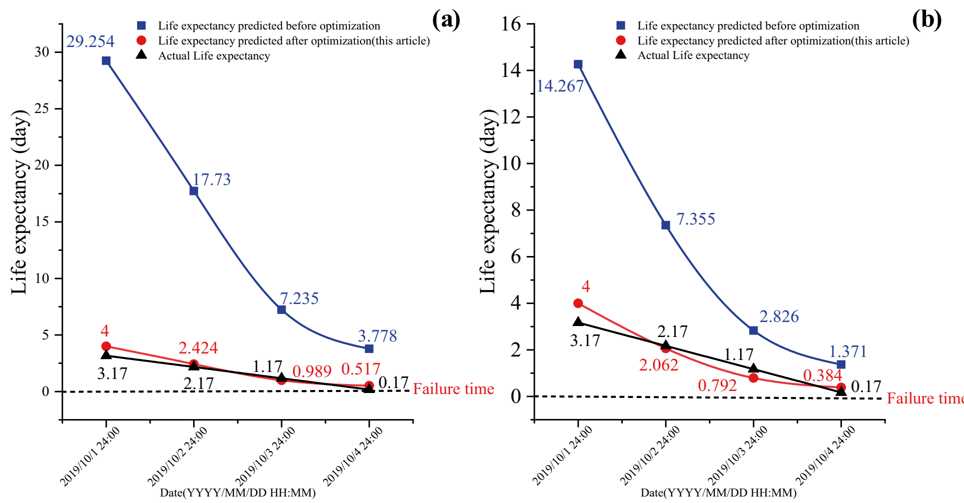

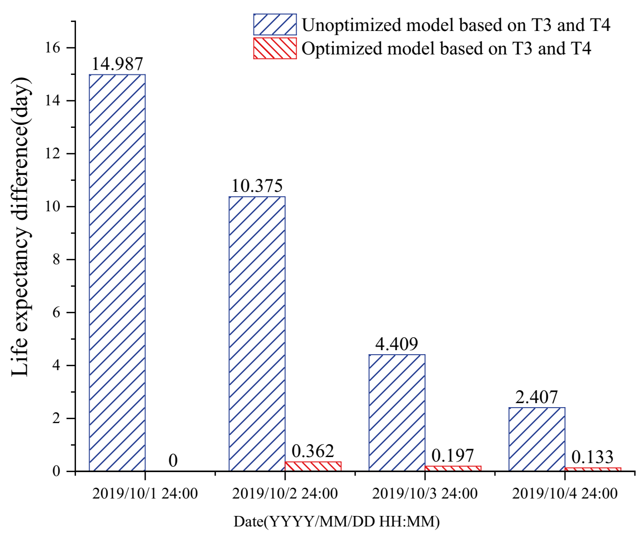

Fig. 14 Life expectancy difference based on the T3 and T4 nodes

Taking October 4, 2019, for example, the life expectancy predicted based on the T3 node and the T4 node differed by 2.407 days in the unoptimized model. In the optimized model, the difference in the life expectancy predicted based on the two monitoring points is 0.133 days. The above data analysis shows that compared with the existing early warning model, the optimized model has better adaptability to different monitoring points.

Conclusions

In this study, we deployed the wireless tilting sensor network to monitor the tilting rate of the Dangchuan section in the Heifangtai region to explore whether the inclination of the slope surface can be used as a landslide warning parameter.

By analyzing the inclination angle data when the actual landslide occurred, we found that the tilting angle of the slope surface changed significantly near the time when the landslide occurred, which is on-site direct evidence for warning the landslides with angle tilting. Thus, it is feasible to use tilt angle change as a landslide warning parameter.

Furthermore, we used the monitoring data to verify the tilting angle early warning model that Xie proposed, and found that the early warning time in his model was much longer than the landslide occurrence time, the early warning time range was too large, and the early warning was not timely enough. In this article, we optimize *B* value in the model proposed by Xie so that *B* contains the rate change characteristics of the acceleration phase of the landslide at the monitoring point. By substituting the monitored data into the optimized model, we found that the optimized model can shorten the early warning time range. In addition, the early warning time of different monitoring points is more consistent, which improves the timeliness of early warning. Therefore, it is proved that the tilting angle can be used for early warning at actual landslide sites.

It should be pointed out that this method still has some limitations and needs to be improved.

(1) In this case, we only deployed two tilting sensors to obtain the loess landslide surface tilt change. The monitoring data is limited in spatial scale. So we cannot give a conclusion that tilting is induced by the sliding kinematic or by wetting-induced pre-failure deformation. In order to find this answer, we need to deploy more tilting sensors to establish a wireless tilting sensor network.

(2) The readings of the tilting sensor nodes, in this case, cannot correlate with the possible slip surface. In order to make the tilting state correspond to the sliding surface, it is necessary to install inclination sensors on different sliding surfaces in the landslide body for measurement. In order to maintain the effectiveness of the method proposed in this paper, we need a wireless underground communication technology to establish a wireless data link for angle sensor nodes in different formations (Wang et al. 2021), and a large amount of angle data is used to judge the potential slip surface.

Acknowledgements

The authors would like to thank graduate students Tianxiang Zhuo, Dingkang Zou, and Chaoyu Wei for their help during the deployment of the system. We also want to give great thanks to Wisen Innovation Company, Wuxi, China, for offering the Wisen wireless sensor system.

Funding

This work was sponsored by the National Natural Science Foundation of China (41521002), the State Key Laboratory of Geohazard Prevention and Geoenvironment Protection Independent Research Project (SKLGP2019Z012), and the Sichuan Science and Technology Program (2021YFS0324). It was also partially supported by the China Scholarship Council (201808510005).

References

Brabb EE (1991) The world landslide problem. Episodes 14:52–61. https://doi.org/10.18814/epiiugs/1991/v14i1/008

Fan X, Xu Q, Liu J et al (2019) Successful early warning and emergency response of a disastrous rockslide in Guizhou Province, China. Landslides 16:2445–2457. https://doi.org/10.1007/s10346-019-01269-6

Lin M, Yan W, Wassell I (2008) Wireless sensor network: water distribution monitoring system. In: Radio & Wireless Symposium. IEEE. https://doi.org/10.1109/RWS.2008.4463607

Liu Y, Liao M, Shi X et al (2016) Potential loess landslide deformation monitoring using L-band SAR interferometry. Geo-Spatial Inf Sci 19:273–277. https://doi.org/10.1080/10095020.2016.1258202

Lu GY, Chiu LS, Wong DW (2007) Vulnerability assessment of rainfall-induced debris flows in Taiwan. Nat Hazards 43(2):223–244. https://doi.org/10.1007/s11069-006-9105-y

Nadim F, Kjekstad O, Peduzzi P et al (2006) Global landslide and avalanche hotspots. Landslides 3:159–173. https://doi.org/10.1007/s10346-006-0036-1

Pecoraro G, Calvello M, Piciullo L (2018) Monitoring strategies for local landslide early warning systems. Landslides 16:213–231. https://doi.org/10.1007/s10346-018-1068-z

Peng J, Lin H, Wang Q et al (2014) The critical issues and creative concepts in mitigation research of loess geological hazards. J Engingeering Geol 22:684–691. https://doi.org/10.13544/J.CNKI.JEG.2014.04.014

Qi X, Xiu D, Peng D, Ju Y (2018) Forecasting method of sliding distance of static liquefaction-type loess landslide in Heifangtai, Gansu Province. J Sichuan Univ Sci Eng (Natural Sci Ed) 31(4):83–88. https://doi.org/10.11863/j.suse.2018.04.13

Qi X, Xu Q, Li B et al (2016) Preliminary study on mechanism of surface water infiltration at Heifangtai loess landslide in Gansu. J Eng Geol 24(3):418–424. https://doi.org/10.13544/j.cnki.jeg.2016.03.011

Robinson G, Spieker A (1978) Nature to be commanded…: earth-science maps applied to land and water management

Uchimura T, Towhata I, Lan Anh TT et al (2010) Simple monitoring method for precaution of landslides watching tilting and water contents on slopes surface. Landslides 7:351–357. https://doi.org/10.1007/s10346-009-0178-z

Uchimura T, Towhata I, Wang L et al (2015) Precaution and early warning of surface failure of slopes using tilt sensors. Soils Found 55(5):1086–1099. https://doi.org/10.1016/j.sandf.2015.09.010

Wang H, Zhuo T, Zhong P et al (2021) A novel wireless underground transceiver for landslide internal parameter monitoring based on magnetic induction. Int J Circuit Theory Appl 1–10. https://doi.org/10.1002/cta.2975

Xie J, Uchimura T, Wang G et al (2020) A new prediction method for the occurrence of landslides based on the time history of tilting of the slope surface. Landslides 17:301–312. https://doi.org/10.1007/s10346-019-01283-8

Xu Q, Peng D, He C, et al (2020) Theory and method of monitoring and early warning for sudden loess landslide—a case study at Heifangtai terrace. J Eng Geol 28:111–121 (in Chinese). https://doi.org/10.13544/J.CNKI.JEG.2019-038

Yue J (2014) Research on railway slope monitoring and early warning based on instrument for surface inclined deformation. Shijiazhuang Tiedao University. (in Chinese)

Zhao C, Zhang Q, He Y et al (2016) Small-scale loess landslide monitoring with small baseline subsets interferometric synthetic aperture radar technique—case study of Xingyuan landslide. Shaanxi, China J Appl Remote Sens, pp 10–026030. https://doi.org/10.1117/1.JRS.10.026030

Honghui Wang (✉) · Pan Zhong · Qiang Xu
State Key Laboratory of Geohazard Prevention and Geoenvironment Protection, Chengdu University of Technology, Chengdu 610059, People's Republic of China
Email: wanghh@cdut.edu.cn

Honghui Wang · Yunshun Zhong
Department of Civil and Environmental Engineering, University of California At Berkeley, Berkeley, CA 94720, USA

Honghui Wang
Email: wanghh@cdut.edu.cn

Yunshun Zhong
Email:zys@berkeley.edu

Dehao Xiu
School of College of Environment and Civil Engineering,
Chengdu University of Technology, Chengdu 610059,
People's Republic of China
Email: xiu.dehao@qq.com

Dalei Peng
Department of Civil and Environmental Engineering, The Hong Kong
University of Science and Technology, Hong Kong, China
Email: pengdalei@ust.hk